Current Biology 22, 1990–1997, November 6, 2012 ©2012 Elsevier Ltd All rights reserved http://dx.doi.org/10.1016/j.cub.2012.08.049

Article

STIM1 Juxtaposes ER to Phagosomes, Generating Ca^{2+} Hotspots that Boost Phagocytosis

Paula Nunes,[1] Daniela Cornut,[1] Vanessa Bochet,[2] Udo Hasler,[1,3] Masatsugu Oh-Hora,[4] Jean-Marc Waldburger,[2] and Nicolas Demaurex[1,*]
[1]Department of Cell Physiology and Metabolism
[2]Department of Pathology and Immunology
[3]Department of Medical Specialties
University of Geneva, 1211 Geneva 4, Switzerland
[4]Department of Cell Signaling, Tokyo Medical and Dental University, Yushima, Bunkyo-ku, Tokyo 113-8549, Japan

Summary

Background: Endoplasmic reticulum (ER) membranes are recruited to phagosomes, but the mechanism and functional significance of this ER recruitment is not known. Here, we show that the ER Ca^{2+} sensor stromal interaction molecule 1 (STIM1) sustains high-efficiency phagocytosis by recruiting thin ER cisternae that interact productively but do not fuse with phagosomes.
Results: Endogenous STIM1 was recruited to phagosomes upon ER Ca^{2+} depletion in mouse neutrophils, and exogenous YFP-STIM1 puncta coincided with localized Ca^{2+} elevations around phagosomes in fibroblasts expressing phagocytic receptors. STIM1 ablation decreased phagocytosis, ER-phagosome contacts, and periphagosomal Ca^{2+} elevations in both neutrophils and fibroblasts, whereas STIM1 re-expression in *Stim1*$^{-/-}$ fibroblasts rescued these defects, promoted the formation and elongation of tight ER-phagosome contacts upon ER Ca^{2+} depletion and increased the shedding of periphagosomal actin rings. Re-expression of a signaling-deficient STIM1 mutant unable to open Ca^{2+} channels recruited ER cisternae to the vicinity of phagosomes but failed to rescue phagocytosis, actin shedding, and periphagosomal Ca^{2+} elevations. The periphagosomal Ca^{2+} hotspots were decreased by extracellular Ca^{2+} chelation and by Ca^{2+} channels inhibitors, revealing that the Ca^{2+} ions originate at least in part from phagosomes.
Conclusions: Our findings indicate that STIM1 recruits ER cisternae near phagosomes for signaling purposes and that the opening of phagosomal Ca^{2+} channels generates localized Ca^{2+} elevations that promote high-efficiency phagocytosis.

Introduction

Phagocytosis is a fundamental cellular event of great clinical relevance, and many microorganisms disrupt intracellular signals controlling phagocytosis to evade destruction by innate immune cells [1]. In neutrophils, Ca^{2+} elevations boost phagocytosis by promoting phagolysosome fusion [2], shedding of the actin coat [3], and NAPDH oxidase activation [4], but the mechanism driving localized Ca^{2+} elevations around phagosomes [5] remains elusive [6]. Stromal interaction molecule 1 (STIM1) was recently identified as a ubiquitous ER Ca^{2+} sensor that, upon Ca^{2+} depletion of the ER, induces the formation near the plasma membrane (PM) of thin ER cisternae known as cortical ER [7]. STIM1 molecules on the cortical ER interact with store-operated Ca^{2+} entry (SOCE) channels on the PM, sustaining long-lasting Ca^{2+} signals required for the activation of T cells [8]. ER remodeling is a prominent feature of phagocytosis whose functional significance was much debated. Although ER recruitment to phagosomes had been previously shown [9], more in-depth studies proposed that the ER provided membranes to phagosomes and supplied ER resident proteins for antigen cross-presentation [10, 11]. However, because these functions require the ER to fuse with phagosomes, these proposals were strongly contested [12]. Whether STIM1-mediated ER remodeling occurs during phagocytosis is not known, but engagement of phagocytic receptors releases Ca^{2+} from internal stores [6] and the ER structures accumulating near phagosomes bear a striking similarity to the cortical ER structures induced by STIM1. Furthermore, STIM1 ablation decreases phagocytosis in mouse peritoneal macrophages [13] and STIM1 knockdown reduces intraphagosomal ROS production in HL60 cells [14]. We therefore postulated that STIM1 could recruit ER cisternae to phagosomes for signaling purposes and confirmed this by light and electron microscopy by comparing wild-type (WT) fibroblasts to fibroblasts from STIM1 knockout mice rendered phagocytic by expression of FcγRIIA receptors, and WT neutrophils to neutrophils from mice bearing a myeloid-specific ablation of the STIM1 gene. By re-expressing a signaling-deficient STIM1 mutant, we further show that STIM1 interacts with Ca^{2+} channels on phagosomes to promote localized Ca^{2+} elevations that drive periphagosomal actin shedding and high-efficiency phagocytosis.

Results

STIM1 Is Recruited to Nascent Phagosomes

To test whether STIM1 is recruited to phagosomes, we assessed the intracellular location of endogenous and exogenous STIM1 in mouse neutrophils and promyeloid leukemia dHL60 cells ingesting IgG-opsonized sheep red blood cells (RBC) and zymosan particles (Zym), respectively, and in mouse embryonic fibroblasts (MEFs) derived from *Stim1*$^{-/-}$ knockout (STIM1 KO) mice and rendered phagocytic by ectopic expression of FcγRIIA receptors. YFP-STIM1 localized to nascent phagosomes in dHL60 cells (Figure 1A), as early as just before cup closure, with dynamic puncta observed up to 15 min postingestion (see Movie S1 available online).

In phagocytic MEFs, mCherry-STIM1 puncta were observed in close proximity to the FcγRIIA-GFP signal lining the phagosomal membrane (Figure 1B), confirming that the STIM1 molecules accumulated around phagosomes. The phagocytic KO MEFs completely lacked STIM1 but had normal levels of STIM2 (Figure S1A) and exhibited a near complete SOCE defect that was restored by STIM1 re-expression (Figure S1B). STIM1-containing cortical-ER junctions are specialized ER subdomains connected to the bulk ER by a constriction capable of excluding "classic" ER markers such as BiP, a KDEL-containing protein [7]. Phagosomes in MEFs were not decorated by the ER resident protein GFP-KDEL (Figure S1C),

*Correspondence: nicolas.demaurex@unige.ch

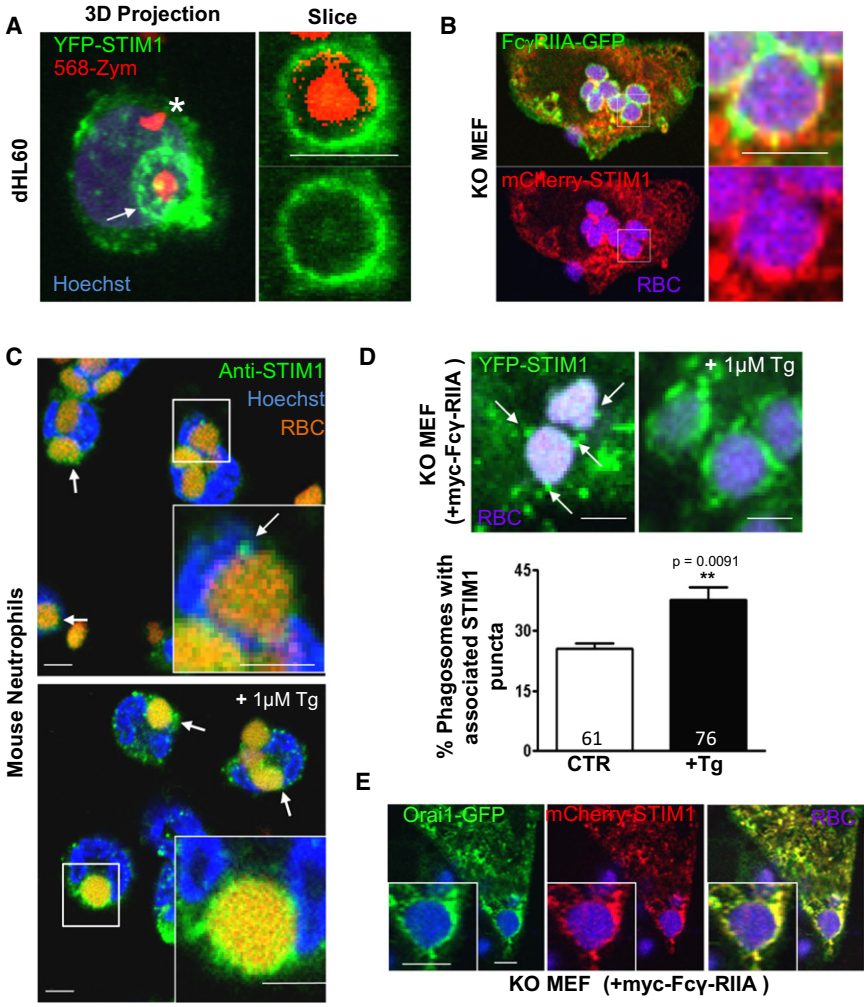

Figure 1. STIM1 Is Recruited to Phagosomes upon Ca^{2+} Depletion of the ER

(A) 3D projection of a confocal z stack shows that YFP-STIM1 (green) is recruited to zymosan-containing phagosomes (red) in dHL60 cells. STIM1 accumulates around nascent phagosomes (arrow) and is shed from mature phagosomes (star). Right-hand zoom represent single-plane confocal slices. See also Movie S1.

(B) Similar to dHL60, mCherry-STIM1 (red) localizes near phagosomes (blue) when re-expressed in STIM1 KO MEFs expressing FcγRIIA-GFP receptors (green).

(C) Endogenous STIM1 (green) staining near phagosomes (red, arrows) is enhanced by ER Ca^{2+} depletion (1μM Tg) in mouse neutrophils.

(D) ER Ca^{2+}depletion (1μM Tg) increases STIM1 (green) recruitment (arrows) to phagosomes (blue) in STIM1 KO MEFs expressing phagocytic receptors.

(E) mCherry-STIM1 (red) colocalizes with its partner channel Orai1-GFP (green) on phagosomes (blue). See also Figure S1. Scale bars represent 3 μm. Data are means ± SEM of three independent experiments, and numbers in bars indicate the total number of measured phagosomes.

indicating that STIM1 was indeed enriched in specialized periphagosomal ER domains. In mouse neutrophils, STIM1 immunoreactive puncta were detected around phagosomes and their numbers increased upon treatment with thapsigargin (Tg, Figure 1C), a SERCA pump inhibitor that increases STIM1 oligomerization and activation by depleting ER Ca^{2+} stores [8]. ER Ca^{2+} depletion also increased the number and size of periphagosomal STIM1 puncta as well as the percentage of phagosomes associated with STIM1 clusters in STIM1-rescued phagocytic MEFs (Figure 1D). Because sorting of plasma membrane proteins into phagosomes occurs even before phagosome closure [15, 16], we then needed to check whether Ca^{2+}-permeable channels gated by STIM1 can be incorporated into phagosomes. All three Orai isoforms localized to phagosomes when expressed in phagocytic MEFs and dHL60 (Figure S1D), and mCherry-STIM1 colocalized with GFP-tagged Orai1 in these periphagosomal structures (Figure 1E). These data indicate that STIM1 is recruited to nascent phagosomes upon store depletion together with its partner channel Orai1, the major SOCE channel of immune cells.

STIM1 Promotes the Formation of Tight Phagosomal-ER Junctions

Because we were unable to find a good marker for immunostaining the specialized ER subdomains generated by STIM1, we next confirmed that STIM1 indeed recruits ER cisternae to phagosomes by morphological examination, using electron microscopy. ER membranes appeared as dark flattened cisternae, located close to phagosomal membranes in ~37% of phagosomes from WT MEFs, a percentage that dropped to 10% upon STIM1 ablation (Figure 2A). The residual periphagosomal ER structures forming in STIM1-deficient cells were similar in length to those found in WT MEFs, and STIM1 re-expression augmented both their frequency and length by ~70% (Figure 2A). The periphagosomal ER structures were still connected with conventional ER cisternae (Figure S2A) and were detected already at the cup stage (Figure S2B), consistent with dHL60 live-cell imaging. Importantly, ER Ca^{2+} depletion dramatically increased the frequency and length of periphagosomal ER cisternae in WT as well as STIM1-Rescued, but not in KO cells (Figure 2A, right). To test whether endogenous STIM1 also recruits thin ER cisternae near phagosomes in neutrophils, we bred floxed *Stim1$^{fl/fl}$* mice to *LysM-Cre$^{ki/ki}$* knockin mice to restrict STIM1 ablation to myeloid cells and avoid the perinatal death associated with whole-animal STIM1 ablation in mice [17]. STIM1 expression was reduced by ~90% in bone-marrow derived neutrophils isolated by FACs sorting (Figure S2C) from *Stim1$^{fl/fl}$, LysM-Cre$^{ki/ki}$* mice compared to *Stim1$^{+/+}$ LysM-Cre$^{ki/ki}$* littermates (Figures S2D and S2E). ER cisternae juxtaposed to phagosomes were observed in 50% of phagosomes from control neutrophils, a proportion that decreased to 30% in neutrophils from *Stim1$^{fl/fl}$, LysM-Cre$^{ki/ki}$* mice (Figure 2B). The juxtaposed ER cisternae were slightly, but not significantly, shorter in STIM1-ablated neutrophils (Figure 2B), and their frequency and length did not increase upon ER Ca^{2+} stores depletion in either genotype (data not shown). Because periphagosomal STIM1 puncta increased upon Tg

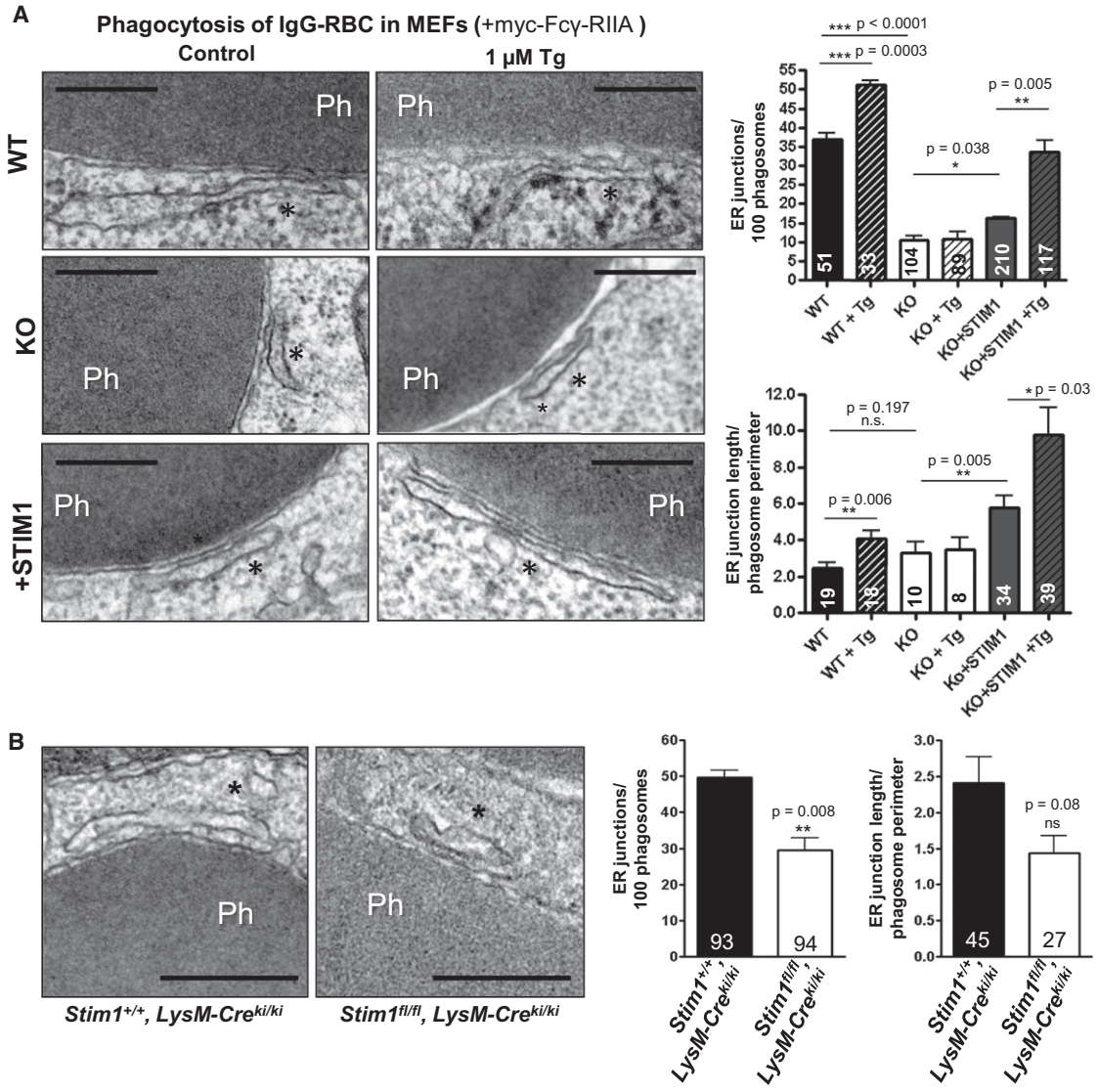

Figure 2. STIM1 Promotes the Formation of Tight Phagosomal-ER Junctions

(A) Electron micrographs illustrating ER cisternae (*) juxtaposed to phagosomes (Ph) in STIM1 WT (top), KO (middle), and STIM1-rescued phagocytic MEFs (bottom) treated or not with 1 μM Tg. Note the long periphagosomal cisternae in STIM1-rescued cells treated with Tg (bottom right). Bar graphs: Quantitative EM analysis shows that STIM1 ablation decreases the frequency (top) and length (bottom) of phagosomal-ER contacts whereas STIM1 rescue increased their occurrence and promoted their formation and elongation upon ER Ca^{2+} depletion.

(B) Myeloid-specific STIM1 ablation decreased the number of periphagosomal ER cisternae (*) in mouse neutrophils without significantly decreasing their length. See also Figure S2. Scale bars represent 200 nm. Data are means ± SEM of three independent experiments, with the total number of measured phagosomes indicated in bars.

addition (Figure 1C), this finding suggests that store depletion either increases STIM1 immunoreactivity or recruits additional STIM1 molecules to already docked ER cisternae in neutrophils. The high levels of ER-phagosome contacts in neutrophils (which are similar to WT MEFs stimulated with Tg), combined with their insensitivity to ER Ca^{2+} depletion suggest that the ER is very efficiently recruited during phagocytosis in these professional phagocytes. Together, these EM data indicate that ER-phagosomal contacts can form in STIM1-deficient cells irrespective of Ca^{2+} store depletion but that STIM1 expression is required for the store-operated recruitment and elongation of ER cisternae to nascent phagosomes.

STIM1 Enhances Phagocytosis and Promotes Phagosomal Actin Shedding

To determine whether STIM1-mediated ER recruitment has a functional impact on phagocytosis, we determined the ability of WT and STIM1 KO MEFs to ingest IgG-opsonized RBCs, using cells with matching FcγRIIA-GFP fluorescence to ensure similar amounts of phagocytic receptors. While WT and KO cells exposed to a low target:cell ratio phagocytosed to a similar extent, increasing the target:cell ratio revealed a defect in phagocytic ingestion of ~30% in KO cells (Figure 3A). Concordantly, when YFP-STIM1 or mCherry-STIM1 (see below) were re-expressed in KO MEFs expressing myc-FcγRIIA, phagocytosis at a high target:cell

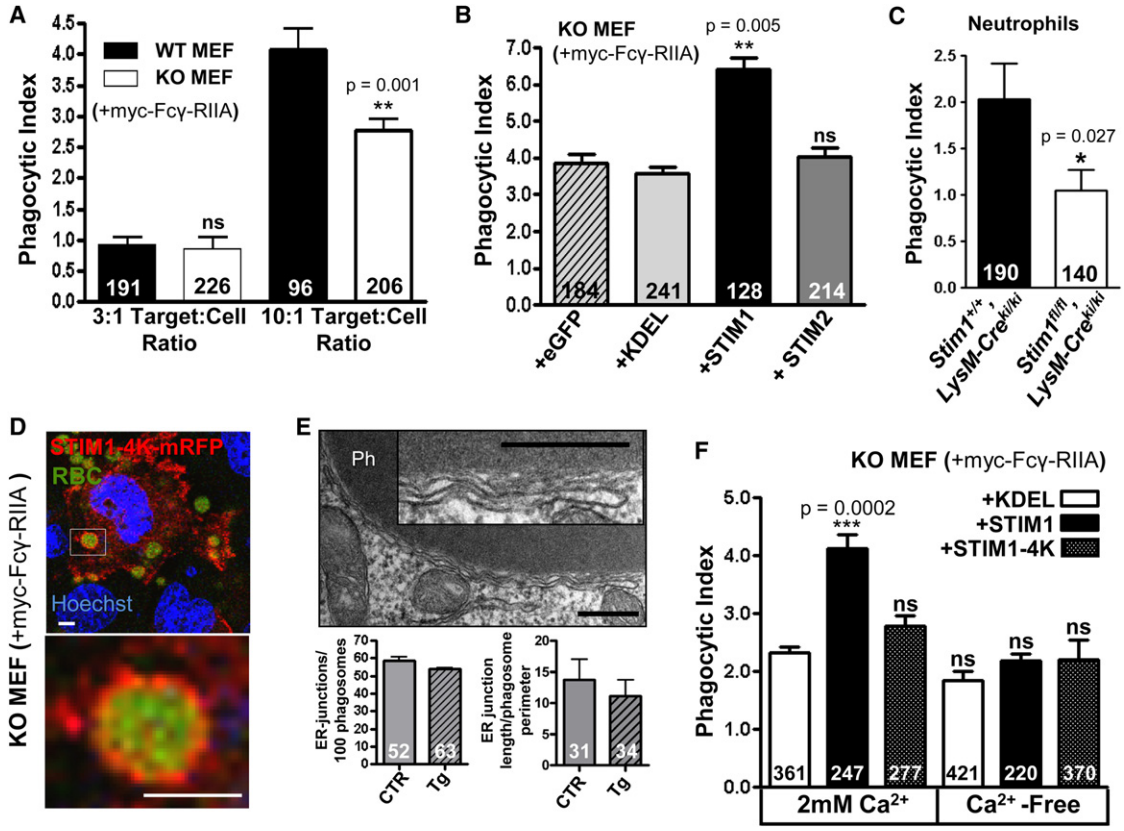

Figure 3. STIM1-Mediated SOCE Channel Activation Is Required for High-Level Phagocytosis

(A) STIM1 ablation decreased phagocytosis at high but not low target loads in MEFs expressing matching levels of FcγRIIA-GFP receptors (n = 3).

(B) YFP-STIM1 but not YFP-STIM2 or ER-targeted KDEL-GFP enhances phagocytosis in STIM1 KO MEFs expressing myc-FcγRIIA receptors (n = 4, 10:1 target:cell ratio).

(C) Myeloid-specific STIM1 ablation reduces phagocytosis by 50% in mouse neutrophils (n = 6, 10:1 target:cell ratio).

(D) STIM1-4K-mRFP lacking polybasic residues (red) required for channel activation is recruited to phagosomes (green). Scale bar represents 3 μm.

(E) STIM1-4K-mRFP promotes the formation and elongation of tight phagosomal-ER contacts (compare with Figure 2A). Ph, phagosome; scale bar represents 200 nm.

(F) STIM1-4K-mRFP does not enhance phagocytosis and removal of extracellular Ca^{2+} abrogates mCherry-STIM1 prophagocytic effects (n = 4, 10:1 target:cell ratio). Data are means ± SEM of 3–6 independent experiments, and numbers in bars indicate total measured cells (A, B, C, F) or phagosomes (E).

ratio was ~40% higher than in cells expressing either cytoplasmic eGFP, ER-targeted KDEL-GFP, or YFP-STIM2 (Figure 3B). These data indicate that although STIM1 is not required for basal levels of particle ingestion, it facilitates phagocytosis as the particle load increases, and that this effect is specific for STIM1. Myeloid-specific STIM1 ablation reduced phagocytosis by nearly 50% in mouse neutrophils (Figure 3C), indicating that endogenous STIM1 also sustains high-level phagocytosis in professional phagocytes. To test whether the prophagocytic effects of STIM1 require productive interactions at the ER-phagosome interface, we expressed a STIM1 mutant lacking the polybasic domain required for Orai channel activation [18] that did not trigger SOCE in MEFs (Figure S1B). This "STIM1-4K" signaling-deficient mutant accumulated around phagosomes (Figure 3D) and increased the frequency and length of periphagosomal ER cisternae when expressed in MEFs (Figure 3E). Store depletion did not further increase either parameter, suggesting that ER recruitment may already be maximal in cells expressing the 4K mutant which, by inhibiting Ca^{2+} influx, is expected to inhibit disassembly of STIM1 oligomers [19]. Notably, STIM1-4K expression did not rescue phagocytosis (Figure 3F), indicating that electrostatic interactions between STIM1 and its target channel(s) are required for the prophagocytic function of STIM1. Consistent with activation of Ca^{2+}-permeable channels, STIM1 re-expression did not augment phagocytosis in Ca^{2+}-free physiological saline (Figure 3F).

Because shedding of the actin coat is an early event during phagocytic maturation that is controlled by Ca^{2+} elevations [3] and reduces phagocytic index when impaired [20–22], we next examined whether STIM1 expression impacted periphagosomal actin structures. Periphagosomal actin rings were more prominent in STIM1 KO cells expressing KDEL-GFP or YFP-STIM1-4K than in cells expressing YFP-STIM1 (Figure 4A), and fluorescence quantification showed that re-expression of WT STIM1, but not of signaling-deficient STIM1-4K, decreased periphagosomal filamentous (F)-actin content, in experiments where STIM1-YFP puncta decorated phagosomes to similar extents (Figure 4B).

STIM1 Promotes Periphagosomal Ca^{2+} Elevations

STIM1-mediated Orai1 channel activation restricts Ca^{2+} entry to distinct sites at the PM [23, 24]. However, whether STIM1 is capable of gating Ca^{2+} channels in internal membrane compartments is unknown. To test whether STIM1 also generates Ca^{2+} hotspots around phagosomes, we measured

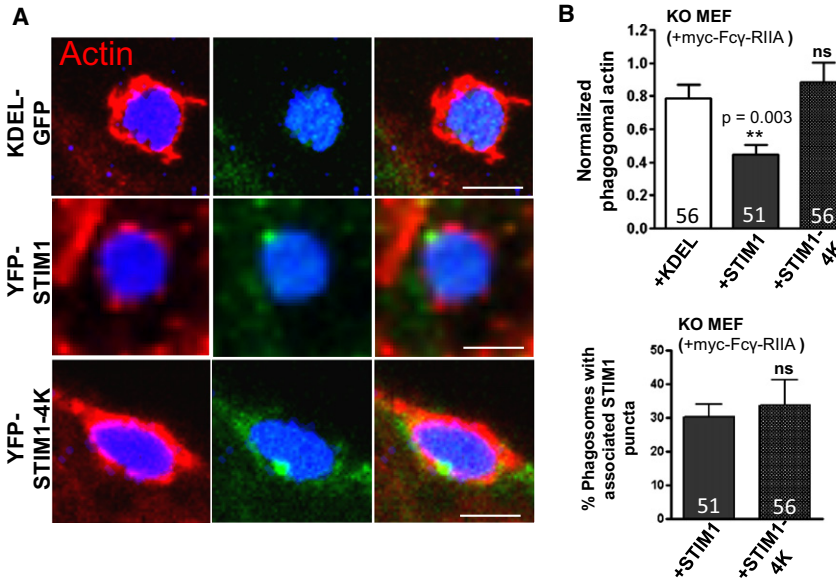

Figure 4. STIM1-Mediated Interactions Promote Periphagosomal Actin Shedding

(A) Periphagosomal F-actin rings (red) were decreased by YFP-STIM1 but not YFP-STIM1-4K re-expression in MEFs.

(B) Average phalloidin intensity in a 1 μm ring surrounding the midsection of phagosomes, normalized to the total cellular phalloidin staining (top) and percentage of phagosomes bearing YFP-STIM1 or YFP-STIM1-4K puncta (bottom). Scale bar represents 3 μm. Data are means ± SEM of four independent experiments, and numbers in bars indicate total measured phagosomes.

Ca^{2+} concentration changes by visualizing cells loaded with the Ca^{2+}-binding dye Fluo8 using confocal microscopy. In MEFs, a low concentration of the Ca^{2+} chelator BAPTA-AM was used to decrease the lateral diffusion of Ca^{2+} and improve hotspots visualization [24]. Ca^{2+} hotspots were observed around ~50% of phagosomes in WT cells, a proportion that decreased to 20% upon STIM1 ablation and that was nearly restored by STIM1 re-expression, whereas STIM1-4K expression increased Ca^{2+} hotspot occurrence only to 28% (Figures 5A and 5B; Table S1). The same hotspot proportion (28%) was observed in STIM1-rescued cells exposed to the SOCE channel inhibitor La^{3+} (5 μM) whereas Ca^{2+} chelation decreased hotspot occurrence to 17% in STIM1-rescued cells (Figure 5B; Table S1). This indicates that periphagosomal ER Ca^{2+} stores and phagosomal Ca^{2+} channels both contribute to the Ca^{2+} hotspots observed in the vicinity of phagosomes, with STIM-gated Ca^{2+} channels contributing more than half of the signal. Periphagosomal Ca^{2+} hotspots were already visible as early as 2 min after particle contact and usually occurred repeatedly at the same location, with some single hotspots persisting for several minutes (Figure 5C; Movie S2). Strikingly, the formation of STIM1 puncta coincided temporally and spatially with the appearance of periphagosomal Ca^{2+} microdomains (Figure 5D; Movie S3), implying that STIM1 recruitment to phagosomes initiates the localized intracellular Ca^{2+} elevations. Periphagosomal Ca^{2+} hotspots coincident with mCherry-STIM1 puncta were also observed in cells treated with 1 μM Tg after switching to Ca^{2+}-free conditions (Movie S4), further validating the phagosomal origin of the Ca^{2+} ions. That STIM1 relies on phagosomal Ca^{2+} and on polybasic residues gating Orai channels to promote both periphagosomal Ca^{2+} hotspots and phagocytosis indicate that the opening of phagosomal SOCE channels is the major mechanism by which STIM1 boosts phagocytosis. In agreement with the results obtained in MEFs, the occurrence of Ca^{2+} hotspots was decreased by ~50% in STIM1-depleted neutrophils, the residual hotspots exhibiting the same amplitude as in WT neutrophils over identical resting cytosolic Ca^{2+} levels (Figure 5E). These data indicate that STIM1 interacts with Ca^{2+} channels on phagosomes via electrostatic interactions, to initiate localized Ca^{2+} elevation in their immediate vicinity.

Discussion

Our data show that the Ca^{2+}-signaling molecule STIM1 recruits the ER to an intracellular target, the phagosome, to promote productive interactions required for high efficiency phagocytosis. STIM1 does not mediate ER-phagosome fusion but generates localized Ca^{2+} elevations required for actin shedding by activating SOCE channels on phagosomes, an activity that was only described at the PM so far. This mechanism likely explains the defective phagocytosis of STIM1 knockout peritoneal macrophages [13] and may contribute to the impaired phagosomal ROS production of dHL60 cells depleted of STIM1 and Orai1 [14]. These earlier studies indicated that STIM1-Orai interactions were important for the phagocytic process but inferred that the interactions occurred at the PM to sustain global Ca^{2+} elevations rather than at the ER/phagosome interface. Our findings that STIM-Orai interactions trigger SOCE across the phagosomal membrane establish STIM1 as a key effector molecule that regulates phagocytosis, clarify a long-standing debate on the function of ER recruitment to phagosomes, and have potential therapeutic implications. Intracellular pathogens like *Mycobacterium tuberculosis* and *Leishmenia* subvert Ca^{2+}-dependent processes to survive phagocytic killing [25] and STIM1 mutations are associated with defective clearance of apoptotic cells in nematodes [26] and with immunodeficiencies in mice and humans [27]. The discovery that SOCE molecules control the highly localized Ca^{2+} signals associated with phagocytosis could therefore provide new potential targets for the treatment of infections caused by intracellular pathogens. It also suggests that defective phagocytosis could be part of the clinical picture of STIM1 dependent immunodeficiencies.

Experimental Procedures

Reagents

STIM1 KO MEFs, generated by targeted gene disruption [28], and WT MEF controls were a kind gift from Dr. Marek Michalak (University of Alberta, Canada). Human FcγRIIA-GFP and c-*myc* constructs were a kind gift from Dr. Sergio Grinstein (University of Toronto, Canada). GFP-tagged Orai1, Orai2, and Orai3 were a kind gift from Drs. Ivan Bogeski and Barbara Niemeyer (Saarland University, Germany). YFP and mRFP-tagged STIM1-4K mutants were a kind gift from Dr. Tamas Balla (National Institute of Child Health and Human Development, Bethesda, USA). Please see Supplemental Information for other reagent sources.

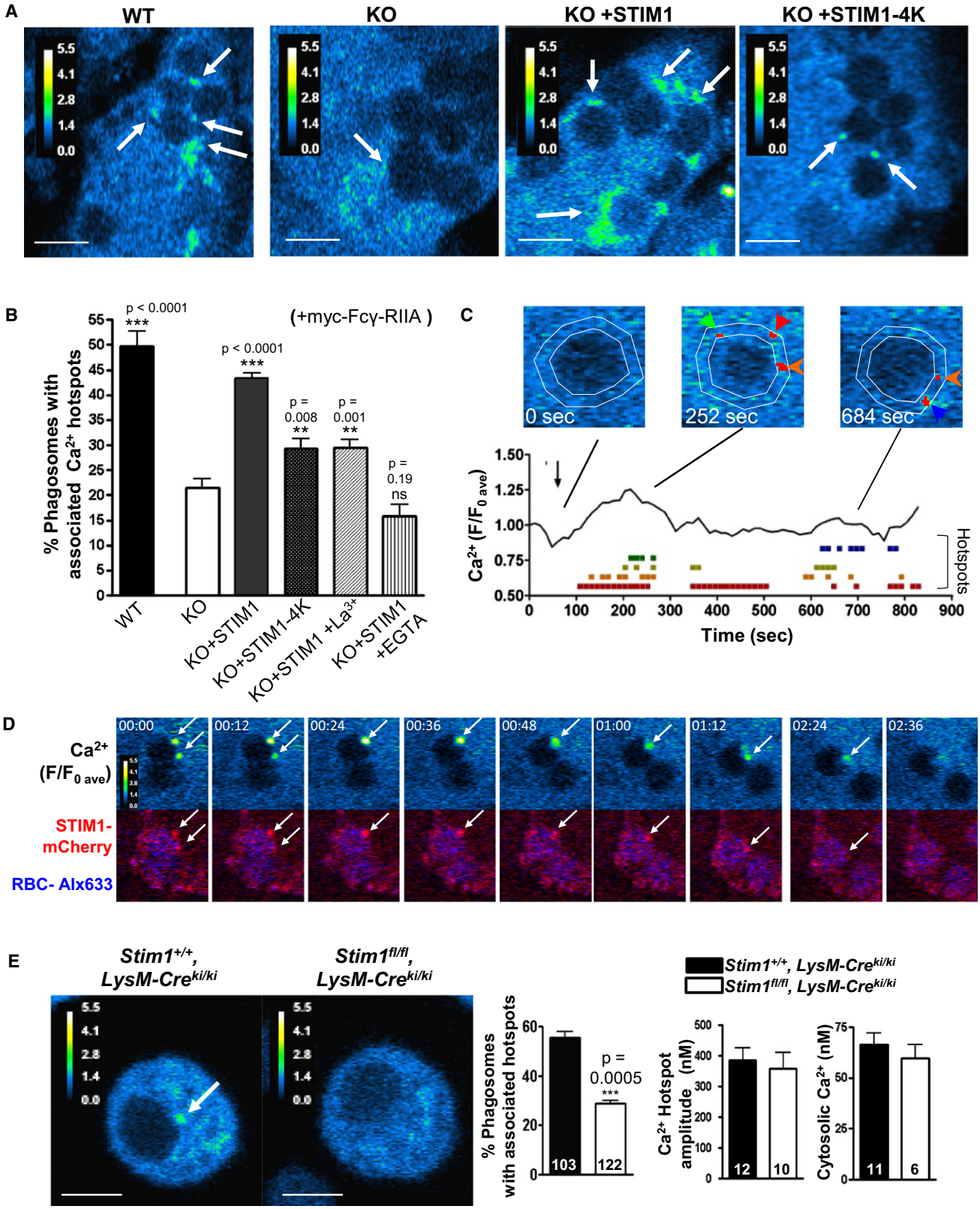

Figure 5. STIM1-Mediated Interactions Promote Periphagosomal Ca^{2+} Signaling

(A) The occurrence of periphagosomal Ca^{2+} elevations was decreased by STIM1 ablation and restored by STIM1 re-expression, whereas STIM1-4K has a smaller effect (arrows, see also quantification in B).

(B) Inhibition of SOCE channels with 5 μM $LaCl_3$ and extracellular Ca^{2+} chelation with 3 mM EGTA reduces periphagosomal Ca^{2+} microdomains in STIM1-rescued cells to levels similar to that of STIM1-4K rescued and KO cells, respectively. See also Table S1.

Cell Culturing and Transfection

MEFs were transfected using Lipofectamine 2000. HL60 cells were differentiated by exposure to 1.3% DMSO for 6 days (dHL60) and transfected using the Amaxa T Nucleofection kit. Transfected cells were allowed to recover for 24 hr prior to manipulation. Please see Supplemental Experimental Procedures for details.

Generation of Myeloid-Specific STIM1 Ablation and FACs Sorting

Mice deficient for STIM1 in the myeloid lineage were generated by crossing *Stim1*$^{fl/fl}$ animals in the C57BL/6 background [29] with the *LysM-Cre*$^{ki/ki}$ strain [30]. All animal manipulations were performed in accordance to the guidelines approved by the animal research committee at the University of Geneva. Genotyping was performed from tail biopsies as described [29, 31]. Neutrophils were isolated from bone marrow of mouse femurs and tibias using Percoll gradient centrifugation as previously described [32]. For FACs sorting, cells were blocked with anti-mouse-Fc-receptor antibodies for 30 min, and incubated with anti-GR-1-APC and anti B220-FITC on ice for 1 hr in 2% BSA, 20 mM EDTA buffer. Sorting was performed on a FACs Aria I sorter (BD Biosciences, Franklin-Lakes, NJ).

Phagocytosis

RBCs were opsonized in rabbit-anti-sheep RBC and zymosan was opsonized in rabbit-anti-zymosan at 37°C for 1 hr. For MEFs and neutrophils, targets were added directly to coverslips at indicated target:cell ratios. For dHL60s, targets were resuspended with cells at a 10:1 target:cell and centrifuged at 8,000 g for 30 s. Cells were then incubated at 37°C/5% CO_2 for indicated times. All phagocytosis experiments were performed in serum-containing media with the exception of actin experiments and experiments comparing Ca^{2+}-containing and Ca^{2+}-free conditions, where serum-free physiological buffer (please see Supplemental Information) was used instead.

Immunolabelling and Actin Staining

Immunolabelling and actin staining were performed according to standard protocols. Please see Supplemental Information for details.

Imaging

All live-cell imaging microscopes were maintained at 37°C by a microscope temperature control system (Life Imaging Services, Basel, Switzerland) and performed in physiological buffer where Ca^{2+}-free solution contained 1 mM EGTA instead of 2 mM $CaCl_2$. Please see Supplemental Information for microscope details. Fura-2-AM (2 μM) was loaded in physiological buffer +0.02% pluronic and visualized using 340/380 nm alternate excitation and 510 ± 40 nm emission. Frames were acquired every 2 s. Fluo8-AM (4 μM) was loaded in physiological buffer/250 μM sulfinpyrazone at 37°C for 30 min. For MEFs, this was followed by addition of BAPTA-AM (5 μM) and incubation for 30 min at room temperature. For neutrophils, cells were instead incubated for an additional 30 min at room temperature in the presence of 1 μM ER-Tracker Red. Simultaneous excitation at 488, 543 nm, and 650 nm and emission collection in three separate channels for green (Fluo8), red (mCherry or mRFP), and far-red (RBC autofluorescence or RBC-Alexa 633 fluorescence, used to define the phagosomal border) was used. For quantification of periphagosomal Ca^{2+} hotspots, images averaged over 6 s and captured between 20 and 30 min after the addition of IgG coated sRBC were used. For time-lapse imaging of periphagosomal Ca^{2+} hotpsots, cells were imaged only with 488 nm laser light, although red channel emission was also collected. To minimize toxicity, we imaged cells for 30 s at 1 s frame rate during particle addition and then again after 5 min of particle addition at 12 s frame rate for an additional 15 min. For Ca^{2+} chelation and Ca^{2+} channel blocking experiments, 3 mM EGTA or 5 μM $LaCl_3$ were added 1 min prior to addition of particles. Unless otherwise indicated, all images shown represent single-plane confocal slices.

Image Quantification

All images were background subtracted by subtracting the average intensity of a small region of interest (ROI) that does not contain cells from all intensity values in the same image, prior to analysis. Phagocytic index was defined as the number of internalized phagosomes divided by the total number of (transfected where applicable) cells and was determined by counting internalized phagosomes in confocal z stacks encompassing ~1 μm above and below cell monolayers using ImageJ software. FcγRIIA marks the plasma membranes and nascent phagosomes, and internalized particles were easily distinguished in 3D reconstructions. Peripheral phagosomes were deemed internalized if more than 75% of the target surface showed visible FcγRIIA. FcγRIIA-GFP fluorescence was visualized directly and myc-FcγRIIA was visualized by immunostaining. Total FcγRIIA and total F-actin were defined as the average cellular FcγRIIA-GFP or TRITC-phalloidin fluorescence intensity (FI) respectively of 32-bit sum projections of confocal stacks. FcγRIIA-GFP expressing cells were thresholded to ensure populations of similar total FcγRIIA-GFP. Phagosomal F-actin was estimated using a previously described approach [33]. Briefly, the TRITC-phalloidin FI was measured within 1 μm of the phagosomal border (defined using the RBC fluorescence) in single confocal slices sectioning the middle of the phagosome. Normalized phagosomal F-actin is phagosomal F-actin/total F-actin of the same cell. Phagosomal F-actin was quantified for all internalized phagosomes and peripheral phagosomes whose target surface showed more than 50% association with F-actin 10 min after target exposure. At least five confocal stacks of equal dimensions per genotype per experiment and at least three independent experiments were quantified.

In MEFs, periphagosomal Ca^{2+} hotspots were defined as areas ≥500 nm^2 (4 pixels) within a distance of ~750 nm (3 pixels) from the phagosomal border displaying a FI at least 2 SDs higher than the average cytoplasmic Fluo8 FI. For neutrophils, ER-Tracker Red reliably demarcated nonnuclear areas and was less toxic than Hoechst during live imaging and thus was used as guide to avoid the nucleus and areas of ER-associated Ca^{2+} activity when defining cytosolic ROIs. In addition, because in neutrophils BAPTA-AM was not used to increase contrast, a cutoff of 2.5 SD above the mean cytoplasmic Fluo8 FI was used instead. Periphagosomal Ca^{2+} traces were generated by tracking phagosomes with a 3-pixel-wide (~750 nm) periphagosomal ROI in 12 s frame time-lapse series. Tracking began 3 frames prior to phagosome arrival in the plane of focus, and average fluorescence values of the first ROI were used to normalize subsequent values. The SD of this first ROI was used to set a threshold of 2.5 SD to identify hotspots, again defined as being above-threshold regions ≥4 contiguous pixels (~500 nm^2).

All statistical analyses were performed using Prism software (GraphPad, La Jolla, USA). Significance between two sets of experiments was determined using a student's t test, whereas group sets were analyzed using ANOVA and Tukey's post test.

Electron Microscopy and Western Blotting

Electron microscopy and western blot analysis were performed according to standard protocols. Please see Supplemental Information for details.

Supplemental Information

Supplemental Information includes two figures, one table, Supplemental Experimental Procedures, and four movies and can be found with this article online at http://dx.doi.org/10.1016/j.cub.2012.08.049.

Acknowledgments

This study was supported by operating grant N° 310030B_133126 from the Swiss National Science Foundation (to N.D.) and N° 310030_122477

(C) Periphagosomal Ca^{2+} hotspots are detected early during phagocytosis and occur sporadically around phagosomes for up to 15 min. The representative trace is the spatially averaged intensities of an ~750 nm wide periphagosomal circle (illustrated in the insets) normalized to the average cytosolic Fluo8 intensity. Colored dots below the trace represent occurrences of Ca^{2+} hotspots in the measured region, where multiple hotspots occurring at the same time point are represented by different colors (illustrated in the insets by colored arrows and red above-threshold regions). See also Movie S2.

(D) Periphagosomal Ca^{2+} hotspots (top) colocalize spatiotemporally with STIM1 puncta (bottom). Images were acquired 5 min after particle addition. See also Movies S3 and S4.

(E) Myeloid-specific STIM1 ablation reduces the occurrence of periphagosomal Ca^{2+} hotspots (arrow) in mouse neutrophils by 50% without altering their amplitude or the average cytosolic Ca^{2+} concentration. White bars represent 3 μm, and colored bars represent the color-coded Fluo8 fluorescence divided by the initial average cytosolic fluorescence (F/F_{0ave}). Data are means ± SEM of 3–12 independent experiments, and the number of total measured phagosomes is detailed in Table S1 or represented inside bars.

(to J.-M.W.). The graphical abstract contains illustrations made by Servier Medical Art (http://www.servier.fr/servier-medical-art).

Received: May 21, 2012
Revised: August 14, 2012
Accepted: August 23, 2012
Published online: October 4, 2012

References

1. Aderem, A., and Underhill, D.M. (1999). Mechanisms of phagocytosis in macrophages. Annu. Rev. Immunol. *17*, 593–623.
2. Jaconi, M.E., Lew, D.P., Carpentier, J.L., Magnusson, K.E., Sjögren, M., and Stendahl, O. (1990). Cytosolic free calcium elevation mediates the phagosome-lysosome fusion during phagocytosis in human neutrophils. J. Cell Biol. *110*, 1555–1564.
3. Bengtsson, T., Jaconi, M.E., Gustafson, M., Magnusson, K.E., Theler, J.M., Lew, D.P., and Stendahl, O. (1993). Actin dynamics in human neutrophils during adhesion and phagocytosis is controlled by changes in intracellular free calcium. Eur. J. Cell Biol. *62*, 49–58.
4. Dewitt, S., Laffafian, I., and Hallett, M.B. (2003). Phagosomal oxidative activity during beta2 integrin (CR3)-mediated phagocytosis by neutrophils is triggered by a non-restricted Ca2+ signal: Ca2+ controls time not space. J. Cell Sci. *116*, 2857–2865.
5. Sawyer, D.W., Sullivan, J.A., and Mandell, G.L. (1985). Intracellular free calcium localization in neutrophils during phagocytosis. Science *230*, 663–666.
6. Nunes, P., and Demaurex, N. (2010). The role of calcium signaling in phagocytosis. J. Leukoc. Biol. *88*, 57–68.
7. Orci, L., Ravazzola, M., Le Coadic, M., Shen, W.-W., Demaurex, N., and Cosson, P. (2009). From the Cover: STIM1-induced precortical and cortical subdomains of the endoplasmic reticulum. Proc. Natl. Acad. Sci. USA *106*, 19358–19362.
8. Lewis, R.S. (2007). The molecular choreography of a store-operated calcium channel. Nature *446*, 284–287.
9. Stendahl, O., Krause, K.H., Krischer, J., Jerström, P., Theler, J.M., Clark, R.A., Carpentier, J.L., and Lew, D.P. (1994). Redistribution of intracellular Ca2+ stores during phagocytosis in human neutrophils. Science *265*, 1439–1441.
10. Gagnon, E., Duclos, S., Rondeau, C., Chevet, E., Cameron, P.H., Steele-Mortimer, O., Paiement, J., Bergeron, J.J.M., and Desjardins, M. (2002). Endoplasmic reticulum-mediated phagocytosis is a mechanism of entry into macrophages. Cell *110*, 119–131.
11. Houde, M., Bertholet, S., Gagnon, E., Brunet, S., Goyette, G., Laplante, A., Princiotta, M.F., Thibault, P., Sacks, D., and Desjardins, M. (2003). Phagosomes are competent organelles for antigen cross-presentation. Nature *425*, 402–406.
12. Touret, N., Paroutis, P., Terebiznik, M., Harrison, R.E., Trombetta, S., Pypaert, M., Chow, A., Jiang, A., Shaw, J., Yip, C., et al. (2005). Quantitative and dynamic assessment of the contribution of the ER to phagosome formation. Cell *123*, 157–170.
13. Braun, A., Gessner, J.E., Varga-Szabo, D., Syed, S.N., Konrad, S., Stegner, D., Vögtle, T., Schmidt, R.E., and Nieswandt, B. (2009). STIM1 is essential for Fcgamma receptor activation and autoimmune inflammation. Blood *113*, 1097–1104.
14. Steinckwich, N., Schenten, V., Melchior, C., Bréchard, S., and Tschirhart, E.J. (2011). An essential role of STIM1, Orai1, and S100A8-A9 proteins for Ca2+ signaling and FcγR-mediated phagosomal oxidative activity. J. Immunol. *186*, 2182–2191.
15. Mercanti, V., Charette, S.J., Bennett, N., Ryckewaert, J.J., Letourneur, F., and Cosson, P. (2006). Selective membrane exclusion in phagocytic and macropinocytic cups. J. Cell Sci. *119*, 4079–4087.
16. Goodridge, H.S., Reyes, C.N., Becker, C.A., Katsumoto, T.R., Ma, J., Wolf, A.J., Bose, N., Chan, A.S., Magee, A.S., Danielson, M.E., et al. (2011). Activation of the innate immune receptor Dectin-1 upon formation of a 'phagocytic synapse'. Nature *472*, 471–475.
17. Baba, Y., Nishida, K., Fujii, Y., Hirano, T., Hikida, M., and Kurosaki, T. (2008). Essential function for the calcium sensor STIM1 in mast cell activation and anaphylactic responses. Nat. Immunol. *9*, 81–88.
18. Korzeniowski, M.K., Manjarrés, I.M., Varnai, P., and Balla, T. (2010). Activation of STIM1-Orai1 involves an intramolecular switching mechanism. Sci. Signal. *3*, ra82.
19. Shen, W.W., Frieden, M., and Demaurex, N. (2011). Local cytosolic Ca2+ elevations are required for stromal interaction molecule 1 (STIM1) de-oligomerization and termination of store-operated Ca2+ entry. J. Biol. Chem. *286*, 36448–36459.
20. Araki, N., Johnson, M.T., and Swanson, J.A. (1996). A role for phosphoinositide 3-kinase in the completion of macropinocytosis and phagocytosis by macrophages. J. Cell Biol. *135*, 1249–1260.
21. Coppolino, M.G., Dierckman, R., Loijens, J., Collins, R.F., Pouladi, M., Jongstra-Bilen, J., Schreiber, A.D., Trimble, W.S., Anderson, R., and Grinstein, S. (2002). Inhibition of phosphatidylinositol-4-phosphate 5-kinase Ialpha impairs localized actin remodeling and suppresses phagocytosis. J. Biol. Chem. *277*, 43849–43857.
22. Scott, C.C., Dobson, W., Botelho, R.J., Coady-Osberg, N., Chavrier, P., Knecht, D.A., Heath, C., Stahl, P., and Grinstein, S. (2005). Phosphatidylinositol-4,5-bisphosphate hydrolysis directs actin remodeling during phagocytosis. J. Cell Biol. *169*, 139–149.
23. Lioudyno, M.I., Kozak, J.A., Penna, A., Safrina, O., Zhang, S.L., Sen, D., Roos, J., Stauderman, K.A., and Cahalan, M.D. (2008). Orai1 and STIM1 move to the immunological synapse and are up-regulated during T cell activation. Proc. Natl. Acad. Sci. USA *105*, 2011–2016.
24. Luik, R.M., Wu, M.M., Buchanan, J., and Lewis, R.S. (2006). The elementary unit of store-operated Ca2+ entry: local activation of CRAC channels by STIM1 at ER-plasma membrane junctions. J. Cell Biol. *174*, 815–825.
25. Malik, Z.A., Thompson, C.R., Hashimi, S., Porter, B., Iyer, S.S., and Kusner, D.J. (2003). Cutting edge: Mycobacterium tuberculosis blocks Ca2+ signaling and phagosome maturation in human macrophages via specific inhibition of sphingosine kinase. J. Immunol. *170*, 2811–2815.
26. Gronski, M.A., Kinchen, J.M., Juncadella, I.J., Franc, N.C., and Ravichandran, K.S. (2009). An essential role for calcium flux in phagocytes for apoptotic cell engulfment and the anti-inflammatory response. Cell Death Differ. *16*, 1323–1331.
27. Feske, S. (2009). ORAI1 and STIM1 deficiency in human and mice: roles of store-operated Ca2+ entry in the immune system and beyond. Immunol. Rev. *231*, 189–209.
28. Prins, D., Groenendyk, J., Touret, N., and Michalak, M. (2011). Modulation of STIM1 and capacitative Ca2+ entry by the endoplasmic reticulum luminal oxidoreductase ERp57. EMBO Rep. *12*, 1182–1188.
29. Oh-Hora, M., Yamashita, M., Hogan, P.G., Sharma, S., Lamperti, E., Chung, W., Prakriya, M., Feske, S., and Rao, A. (2008). Dual functions for the endoplasmic reticulum calcium sensors STIM1 and STIM2 in T cell activation and tolerance. Nat. Immunol. *9*, 432–443.
30. Clausen, B.E., Burkhardt, C., Reith, W., Renkawitz, R., and Förster, I. (1999). Conditional gene targeting in macrophages and granulocytes using LysMcre mice. Transgenic Res. *8*, 265–277.
31. Lamacchia, C., Palmer, G., Seemayer, C.A., Talabot-Ayer, D., and Gabay, C. (2010). Enhanced Th1 and Th17 responses and arthritis severity in mice with a deficiency of myeloid cell-specific interleukin-1 receptor antagonist. Arthritis Rheum. *62*, 452–462.
32. El Chemaly, A., Okochi, Y., Sasaki, M., Arnaudeau, S., Okamura, Y., and Demaurex, N. (2010). VSOP/Hv1 proton channels sustain calcium entry, neutrophil migration, and superoxide production by limiting cell depolarization and acidification. J. Exp. Med. *207*, 129–139.
33. Serrander, L., Skarman, P., Rasmussen, B., Witke, W., Lew, D.P., Krause, K.H., Stendahl, O., and Nüsse, O. (2000). Selective inhibition of IgG-mediated phagocytosis in gelsolin-deficient murine neutrophils. J. Immunol. *165*, 2451–2457.